CHAPTER 11

Survival prediction model of children with diffuse intrinsic pontine glioma based on clinical and radiological criteria

Jansen MHA, Veldhuijzen van Zanten SEM, Sanchez Aliaga E, Heymans MW, Warmuth-Metz M, Hargrave D, van der Hoeven EJ, Gidding CE, de Bont ES, Eshghi OS, Reddingius R, Peeters CM, Schouten-van Meeteren AYN, Gooskens RHJ, Granzen B, Paardekooper GM, Janssens GO, Noske DP, Barkhof F, Kramm CM, Vandertop WP, Kaspers GJL, van Vuurden DG

Neuro Oncol. 2015;17(1):160–6

ABSTRACT

INTRODUCTION Although diffuse intrinsic pontine glioma (DIPG) carries the worst prognosis of all pediatric brain tumors, studies on prognostic factors in DIPG are sparse. To control for confounding variables in DIPG studies, which generally include relatively small patient numbers, a survival prediction tool is needed. **METHODS** A multicenter retrospective cohort study was performed in the Netherlands, the UK, and Germany with central review of clinical data and MRI scans of children with DIPG. Cox proportional hazards with backward regression was used to select prognostic variables ($P < .05$) to predict the accumulated 12-month risk of death. These predictors were transformed into a practical risk score. The model's performance was validated by bootstrapping techniques. **RESULTS** A total of 316 patients were included. The median overall survival was 10 months. Multivariate Cox analysis yielded 5 prognostic variables of which the coefficients were included in the risk score. Age ≤3 years, longer symptom duration at diagnosis, and use of oral and intravenous chemotherapy were favorable predictors, while ring enhancement on MRI at diagnosis was an unfavorable predictor. With increasing risk score categories, overall survival decreased significantly. The model can distinguish between patients with very short, average, and increased overall survival (medians of 7.0, 9.7, and 13.7 mo, respectively). The area under the receiver operating characteristic curve was 0.68. **DISCUSSION** We developed a DIPG survival prediction tool that can be used to predict the outcome of patients and for stratification in trials. Validation of the model is needed in a prospective cohort.

INTRODUCTION

Pediatric brain tumors comprise 20%–25% of childhood cancer. Among these, diffuse intrinsic pontine glioma (DIPG) carries the worst prognosis [1]. The median overall survival (OS) is 9 months, and ≤10% of patients are alive at 2 years after diagnosis [2,3]. With the introduction of MRI in the 1990s, specific radiological characteristics of brainstem tumors have been associated with prognosis. This led to the important distinction of diffuse gliomas arising in the pons from more focal tumors of the midbrain, cervico-medullary junction, and medulla oblongata that have a better prognosis [4]. Since then, study populations in DIPG trials have been more homogeneous, as the general consensus is to include patients with a T1-hypointense and T2-hyperintense tumor involving ≥50% of the pons, sometimes complemented by the presence of one of the classical triad of symptoms [5].

However, among DIPG study populations, although the long-term outcome is invariably dismal, the median OS varies among studies from 7 to 16 months [2,3]. It is important to know whether these variations are caused by treatment effects or by confounders, as virtually all studies are nonrandomized. To make this distinction in future trials, prognostic factors at diagnosis of DIPG should be identified. Significant prognostic factors can be useful for risk-group adapted therapy and subgroup analysis. Until now, studies have been inconclusive as to whether MRI can predict the prognosis of children with DIPG [6–9]. At diagnosis, clinical factors (like age and symptom duration) have been associated with prognosis [10,11]. These prediction studies, however, included relatively few patients.

This study therefore aims to develop the first multivariable prediction model for DIPG survival based on radiological and clinical variables in a large retrospective, multi-institutional, multinational cohort.

METHODS

Study population

The study cohort consisted of children aged 0–18 years with a DIPG. The availability of a diagnostic MRI for review was mandatory to be included in the study. DIPG was defined as a T1-hypo (or iso) intense and T2-hyperintense tumor involving at least 50% of the pons. The diagnosis was established by an experienced neuroradiologist. A search covering the time period from January 1990 to January 2010 was performed in the database of the Dutch Childhood Oncology Group, as well as in local registries of the Dutch childhood cancer and pediatric radiotherapy centers, the patient registry of Great Ormond Street Hospital (GOSH; London, UK), and the HirnTumor Glioblastoma

Multiforme/High-grade Glioma (HIT-GBM/HGG) database of the GPOH (Gesellschaft für Pädiatrische Hämatologie und Onkologie; Germany, Austria, Switzerland). From the HIT-GBM/HGG only MRI's from the 2004–2010 time period were available for central review. No histological confirmation was required.

The local authorities of the Dutch, German, and UK institutions gave permission to use the anonymized patient data. The study was reviewed by the scientific committee of the Dutch Childhood Oncology Group.

Variables

MRI scans at diagnosis were scored by 3 independent reviewers (M.J., S.V., E.S.) on tumor-specific radiological characteristics. Clinical data, histology (if available), and information on the applied treatment were obtained from the patient charts and from the GOSH and HIT-GBM/HGG databases. Table 1 presents the clinical and radiological variables included in the present analysis. Percentage of the pons involved (50%–67% or 67%–100%) and tumor growth in the medulla and mesencephalon were determined 2-dimensionally on axial and sagittal T2-weighted MRI, while the degree of encasement of the basilar artery was determined on T1-weighted images or fluid attenuated inversion recovery (if available). Ring enhancement was defined as one or more areas of a ring-shaped enhancement with a hypointense center on T1-weighted images after gadolinium administration (Fig. 1). Leptomeningeal dissemination was not included, as most patients did not undergo MRI scanning of the whole neuraxis. As patients received different treatments, we categorized these into either oral or intravenous chemotherapy in addition to radiotherapy (RT). If patients received both oral and intravenous chemotherapy, the therapy was categorized as intravenous chemotherapy.

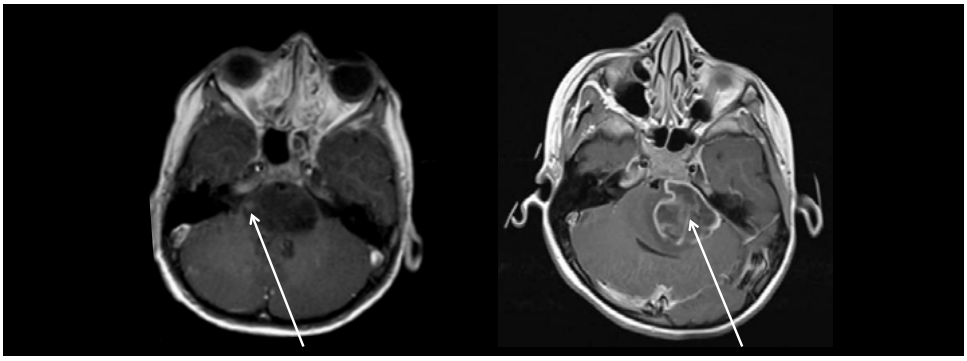

FIGURE 1 | Two patients with DIPG who underwent T1-weighted MRI with contrst: **(A)** the tumor shows a small nodular enhancement (arrow) which was therefore not scored as ring enhancement; **(B)** the tumor shows a large area of ring enhancement (arrow).

TABLE 1 | Baseline characteristics of children with diffuse intrinsic pontine glioma.

Category	Variable	Number (%)
Total		316
Sex	Female	156 (51%)
	Male	160 (49%)
Age	Mean age, y (range)	7.2 (0-18)
	Age <3 y	20 (6%)
Symptom	Mean symptom duration prediagnosis	2.0 (0-30) months
	Symptom duration ≥6 months	21 (7%)
	Symptom duration <6 months	264 (93%)
	Missing	31 (10%)
	Cranial nerve palsy	226 (72%)
	Ataxia	192 (61%)
	Pyramidal tract symptoms	133 (42%)
Histology	WHO II	14 (21%)
	WHO III	21 (31%)
	WHO IV	26 (38%)
	High-grade glioma not defined	7 (10%)
	Unknown (not biopsied)	248 (79%)
MRI	Pontine involvement 50-67%	33 (10%)
	>67%	283 (90%)
	Ring enhancement No contrast given	114 (36%) 14 (4%)
	Encasement basilar artery:	
	180°< encasement <360°	212 (67%)
	Full encasement (360°) No encasement	71 (23%) 33 (10%)
	Hydrocephalus	65 (21%)
	Growth in mesencephalon	183 (58%)
	Growth in medulla oblongata	124 (39%)
Treatment	Radiotherapy	272 (91%)
	Oral chemotherapy[a]	159 (50%)
	Intravenous chemotherapy[b]	33 (10%)
Outcome	Median OS	10 (±0.38) months
	12-mo OS	35%
	24-mo OS	9%
	5-y OS	2%
	Median PFS	6 (±0.25) months

WHO: World Health Organization; PFS: Progression-free survival.

[a] Patients were mainly treated with temozolomide concurrent with and/or adjuvant to RT or with vincristine and carboplatin according to the International Society of Paediatric Oncology low-grade glioma protocol.

[b] HIT-GBM-D: preirradiation methotrexate, radiation, and cisplatin, etoposide, vincristine, and ifosfamide. HITSKK: cyclofosfamide, methotrexate and vincristine or DIPG-VU University Medical Center-1 containting high dose chemotherapy with stem cell reinfusion.

Statistical analysis

Statistical analyses were performed using the SPSS statistical package version 18.0 and R. The cumulative probability of dying before or at 12 months after diagnosis (12-mo risk of death) was chosen as the cutoff, which is commonly used for clinical trials. For development of the prediction model we added all variables with ≤10% missing values to the Cox proportional hazards model; ≥10 (non)events should occur in each variable to be included in the model [12]. Predictors were removed from the model when $P \geq .05$ [13,14]. The regression coefficients from this model were used to obtain the 12-month probability of dying. This probability was calculated using the baseline probability of dying for an individual patient with a follow-up period of 12 months. Next, the patients were categorized into 5 equally sized groups based on these regression coefficients, ranging from low to high. We compared the mean risk of death of each group to the actual survival time of the group using the Kaplan-Meier method.

To test the generalizability of the model, bootstrapping techniques were applied [15], from which 250 new databases were created, each consisting of at least 100 patients randomly selected from the original database. Bootstrapping yielded a shrinkage factor, correcting for overfitting of the model. This shrinkage factor was applied to the regression coefficients before a calibration plot was generated to consider the agreement between predicted and observed probabilities of dying. Subsequently, the area under the receiver operating characteristic (ROC) curve was calculated to test the discriminative ability.

To make our prediction tool suitable for clinical research, each coefficient from the model was transformed to a round number of risk scores. The total risk score for each individual patient could be determined by adding the risk score of each present predictor. The sensitivity, specificity, positive predictive value (PPV), and negative predictive value (NPV) of increasing risk score categories were calculated for the 12-month cumulative risk of death. Finally, we defined 3 risk groups based on the risk score categories and compared them using the Kaplan-Meier method, to obtain information on the predictive capability of the prognostic model beyond 12 months' follow-up.

Subgroup analysis

To investigate whether the model had predictive value in "typical DIPG trial patients", defined as patients aged 3–18 years and treated with RT, we repeated the Cox proportional hazards analysis in this subgroup and performed Kaplan-Meier estimates using the established risk scores.

RESULTS

A total of 316 patients met the inclusion criteria (Table 1); of these, 106 were included from Dutch centers, 65 from GOSH, and 145 from Germany. The median OS of the whole cohort was 10 months, and the 12-month OS was 35%. Males and females were equally represented, and the median age was 7 years. Of all patients, 91% received RT. Patients who did not receive RT were very young, had progressed too fast to receive RT, or had parents who decided not to provide any therapy for their child. Sixty percent of patients received additional chemotherapy: oral chemotherapy in 50% of cases (mostly temozolomide) and intravenous chemotherapy in 10% (Table 1).

Univariate cox proportional hazards analysis

Results of the univariate Cox proportional hazards analysis are shown in Table 2. Age ≤3 years, longer duration of symptoms at diagnosis, and use of oral and/or intravenous chemotherapy all showed a significant correlation with prolonged OS. The presence of ataxia at diagnosis and ring enhancement were negative predictors of OS. None of the variables was excluded from the model based on the outcome of the univariate analysis.

Multivariate cox proportional hazards analysis and development of the prediction model

All variables from the univariate analysis met the inclusion criteria (≤10% missing values and ≥10 events) to be included in the multivariate Cox analysis, except for histology, which was available in only 21% of the patients. Backward selection yielded 5 significant prognostic variables. Based on the regression coefficients of these variables, duration of survival was predicted for all participants. The resulting model consists of positive predictors of prognosis (longer symptom duration, age ≤3 y, and use of oral and intravenous chemotherapy as additive to RT) and one negative predictor (presence of ring enhancement; Table 3). Ataxia was not a significant predictor in the multivariate analysis.

The risk score of a patient is calculated from the coefficients (transformed to a round number) of each predictor (Table 3). For example, a newly diagnosed patient of 8 years of age (+7) with 5 months existing symptoms pre-diagnosis (-5) with a ring-enhancing DIPG (+4), who is not planned to receive chemotherapy in addition to the standard RT, has a total risk score of 6. The predicted risk of death can then be extracted from Table 4: the predicted risk of death for this patient is 74% at 12 months.

TABLE 2 | Results fof the univariate Cox proportional hazards regression analysis.

Baseline variables	Hazard ratio (95% CI)	P
Increasing age, y	1.01 (0.98-1.04)	.68
Age ≥3 y	2.19 (1.25-3.82)	.006
Sex, male vs female	0.92 (0.72-1.17)	.49
Signs and symptoms		
Increasing symptom duration, mo	0.90 (0.86-0.95)	.0001
Cranial nerve palsy	1.29 (0.97-1.70)	.08
Pyramidal tract symptoms	1.18 (0.93-1.50)	.17
Ataxia	1.38 (1.07-1.79)	.02
MRI characteristics		
Pontine involvement: 50-67% vs >67%	1.29 (0.86-1.92)	.21
Ring enhancement	1.53 (1.19-1.97)	.001
Encasement basilar artery:		.49
1) >180°; < 360° vs no encasement	1.15 (0.77-1.73)	
2) 360° vs no encasement	1.30 (0.83-2.05)	
Hydrocephalus	0.95 (0.71-1.28)	.75
Growth in mesencephalon	0.93 (0.73-1.18)	.54
Growth in medulla oblongata	1.17 (0.92-1.48)	.22
Histology		
WHO grade III-IV vs grade II	1.55 (0.80-3.00)	.20
Treatment		
RT + chemotherapy vs RT:		.004
1) Oral chemotherapy	0.64 (0.49-0.84)	
2) Intensive chemotherapy	0.68 (0.45-1.02)	

TABLE 3 | Results of the multivariate Cox proportional hazards analysis and translation into risk score.

Predictor	Hazard ratio (95% CI)	*P*	Coefficient after shrinkage	Contribution to risk score
Age ≥3 y	1.95 (1.01-3.80)	.046	0.667	7
Symptom duration, mo	0.92 (0.86-0.97)	.003	-0.085	-1
Ring enhancement	1.41 (1.07-1.84)	.013	0.354	4
Chemotherapy:		.013		
Oral chemotherapy	0.66 (0.49-0.88)	.048	-0.398	-4
Intensive chemotherapy	0.63 (0.40-0.99)	.047	-0.418	-4

The formula to calculate the DIPG risk score for an individual patient = months of symptom duration (x – 1) + age ≥3y (+7) + ring enhancement (+4) – the use of oral/intensive chemotherapy (=4).

TABLE 4 | Study cohort 12-mo predicted risk of death vs. observed death.

Risk score	Died at 12 Mo *	Censored*	Predicted death	Observed death (KM)
< 1	42	8	0.47	0.40
1 - 2	48	5	0.60	0.60
3 - 5	49	4	0.68	0.63
6	50	1	0.74	0.80
7 - 11	51	2	0.80	0.82

* Number of patients; KM: Kaplan-Meier estimate

The specificity, sensitivity, PPV, and NPV of the risk score on 12-month risk of death are presented in Table 5. Patients with a risk score of <1 had a NPV of 73%; this implies that they had a 27% chance to die within the first 12 months after diagnosis. On the other hand, a patient with a risk score of ≥7 had an 80% chance (PPV at 12 months) to die within 12 months after diagnosis. Internal validation by bootstrapping revealed a 15% overfitting of the model. The predicted and observed probabilities differed by ≤7% (calibration plot after shrinkage is given in Supplementary Fig. 1). The discriminatory capacity of the model was estimated by the area under the ROC curve, which was 0.68 (95%CI: 0.62–0.75) (Supplementary Fig. 2).

TABLE 5 | Study cohort prognostic test characteristics for 12-mo cumulative risk of death.

Risk score	True positive*	True negative*	False positive*	False negative*	Sensitivity	Specificity	PPV	NPV
≥1	118	30	101	11	0.92	0.23	0.50	0.73
≥3	87	73	58	42	0.67	0.56	0.54	0.64
≥6	67	98	33	62	0.52	0.75	0.67	0.61
≥7	20	126	5	109	0.16	0.96	0.80	0.54

* Number of patients

Identification of DIPG risk groups

Figure 2 shows the predictive capability of the risk score over the entire follow-up period. The median OS rates for patients with risk scores of <1, 1–6, and ≥7 were 13.7 (+1.7), 9.7 (+0.4), and 7.0 (+0.9) months, respectively. Therefore, the risk score enables definition of a standard, an intermediate, and a high-risk group within DIPG.

Subgroup analysis (Supplementary data)

The results of the Cox proportional hazards analysis for the sub-group of patients aged 3–18 years who were treated with RT are shown in Supplementary Table 1. The analysis revealed the same predictors as in the original cohort except "age ≤3 years".

Additionally, extension of the tumor in the medulla was a negative predictor in this cohort. Supplementary Figure 3 shows the Kaplan-Meier survival curves when applying the established risk scores to this subgroup. Increasing risk score intervals correlate with decreasing OS; in other words, also within this subgroup a standard, an intermediate, and a high-risk group was identified.

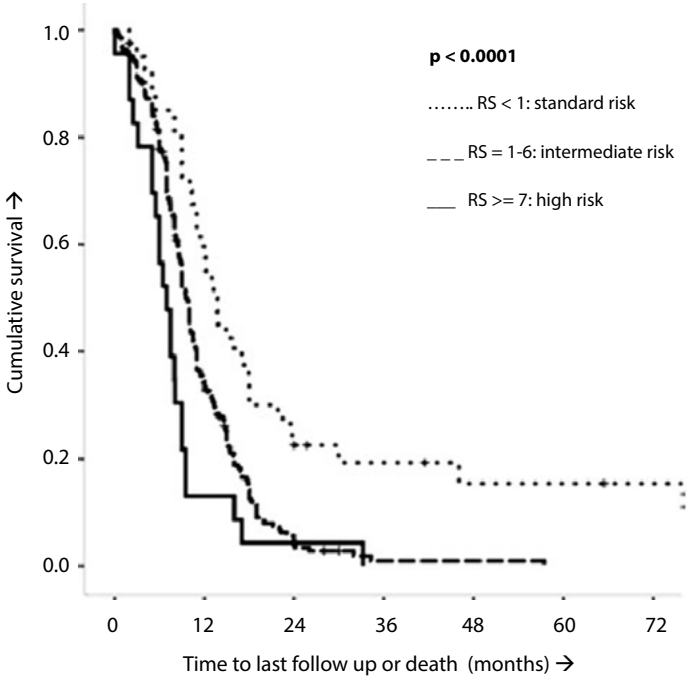

FIGURE 2 | Kaplan-Meier estimates of the DIPG risk score (RS).

Based on the risk score, 3 categories were identified: a standard risk arm (RS <1), an intermediate risk arm (RS 1–6), and a high-risk arm (RS ≥7). The increasing risk arms correlated with decreasing OS time (log-rank $P <$ .0001 and generalized Wilcoxon $P <$ .0001).

DISCUSSION

In this large retrospective cohort study we show that the OS of patients with a DIPG can be predicted at diagnosis by clinical and radiological characteristics, including duration of symptoms, age, and ring enhancement on MRI. We also found chemotherapy to contribute positively to OS, but we cannot exclude that survivorship bias is responsible for this result, as we will discuss later. The combination of these variables results in a DIPG risk score that can be used in future clinical studies. The DIPG risk score predicts the outcome of a study cohort based on standard therapy; thus, the score helps to

conclude whether an apparent change in OS can be attributed to the novel therapeutic intervention or, alternatively, to selection bias. In trials, the DIPG risk score enables stratification of patients into standard, intermediate, and high-risk groups. Our subgroup analysis presented in the Supplementary Data show that the predictors and the DIPG risk score both keep their predictive capacity in the cohort of DIPG patients typically included in trials: those aged 3–18 years and treated with RT. Interestingly, in the whole cohort, the 3-year OS of the high-risk group (risk score ≥7) was 0% versus 20% in the standard risk group (risk score <1). Although this might eventually allow risk-group adapted therapy, because the long-term outcome is currently poor in all 3 groups, it seems that such an approach is not yet indicated in DIPG.

Longer duration of symptoms before diagnosis correlated with improved OS, as previously suggested in a nonmultivariate analysis [11]. Apparently, a less acute presentation reflects a more indolent disease course. In contrast to previous studies, we show the presence of ring enhancement to be a negative predictor of OS. Previous studies did not perform subgroup analyses for specific ring enhancement, and smaller patient numbers were included [6,8]. Our results are in agreement with Poussaint et al. [9] and suggest that ring enhancement matches glioblastoma multiforme histology [9,16]. On the multivariate Cox proportional hazards analysis, we confirmed a survival benefit for patients aged ≤3 years. The cutoff we used was based on 2 reports in which this age group was suggested to have a more favorable prognosis [10,17]. In our and other cohorts, oral and intravenous chemotherapy in addition to RT slightly improved OS in DIPG compared with RT alone [18,19]. However, there are no prospective randomized controlled trials that really prove or disprove a survival benefit for chemotherapy in addition to RT in DIPG. The broad range in median OS (7–16 mo) of all observational, single-arm trials in the past 7 years suggests that there might be an effect of at least some of the drugs, although selection bias cannot be excluded [3,18,19]. In contrast, Cohen et al. [20] reported no survival benefit in a large trial cohort treated with temozolomide, the most commonly used oral drug in DIPG, when compared with a historical DIPG cohort treated with RT only [20]. We are well aware that our results may be biased by survivorship, as patients presented in the RT-only arm may have died too early to receive any further chemotherapy. No further subdivision of specific chemotherapy schedules was possible, since multiple treatments were applied within this cohort, many of them off trial. Obviously, randomized controlled trials are needed to show whether there is a benefit of the addition of chemotherapy to radiotherapy, but it can be questioned whether it is ethical to execute such a randomized study in a population with a dismal prognosis such as DIPG.

With a total of 316 patients, ours is the largest prognostic study in DIPG [4,6–9,11,17,18,21–28]. Another strength of our study is the internal validation of the prognostic model by

bootstrapping. The area under the ROC curve of our model (68%) is modest compared with other diagnostic prediction tests [13,14]. However, prognostic tools are known to achieve lower values [14]. Notably, the curve of the predicted and observed risk of death was well calibrated. The main limitation of the present study is the heterogeneity of treatment regimens applied and the possibility of the previously explained survivorship bias. We included all patients of the participating institutions 1990–2010, on and off trial, and therefore limited the chance of selection bias. However, from the German cohort, only patients diagnosed from 2004 were included, as MRI scans from this time period only could be reviewed.

The presented model is to be validated in a large, prospective, and (preferably) homogeneously treated group of DIPG patients. This will be feasible within the recently initiated European Society of Paediatric Oncology DIPG Network, which created a European DIPG registry of clinical and imaging data (www.dipgregistry.eu), and by use of the International DIPG Registry created in the US (www.dipgregistry.org). In addition, new prognostic variables resulting from other imaging modalities (e.g., MR spectrometry, PET) may be integrated into this model to increase its accuracy [29,30]. Furthermore, with the reintroduction of biopsies into treatment of DIPG, biological predictors may be defined and integrated into the model [31–33]. If, in the near future, studies show that biological features of DIPG are of predictive value and therefore should be used in treatment stratification, this might reinstate biopsy as a common procedure in DIPG therapy. In this respect, it might be worthwhile to investigate in a new study whether long-term survivors cluster in a certain favorable metabolic or molecular profile, such as the recently discovered mutation in the H3.3 histone. Recent published data have suggested that histone mutation status may be prognostic; that is, DIPG tumors expressing wild-type H3.3 showed a more favorable prognosis than those that harbored the H3.3 mutation [32,33].

In conclusion, the present study shows that a risk score based on clinical and radiological variables obtained at diagnosis is able to predict the prognosis of patients with DIPG. Negative predictors were age ≥3 years and the presence of ring enhancement on MRI, whereas longer duration of symptoms at diagnosis was a positive predictor. Furthermore, the use of oral and intravenous chemotherapy contributed positively to survival, although this could be subject to survivorship bias. Our model predicts the outcome of a study cohort treated with standard therapy, thus allowing the possible benefit of a new intervention. In addition, the definition of standard, intermediate, and high-risk groups based on risk score enables stratification of patients in trials, controlling for confounding variables in DIPG. In the future, the model should be validated in a prospective cohort.

SUPPLEMENTARY DATA

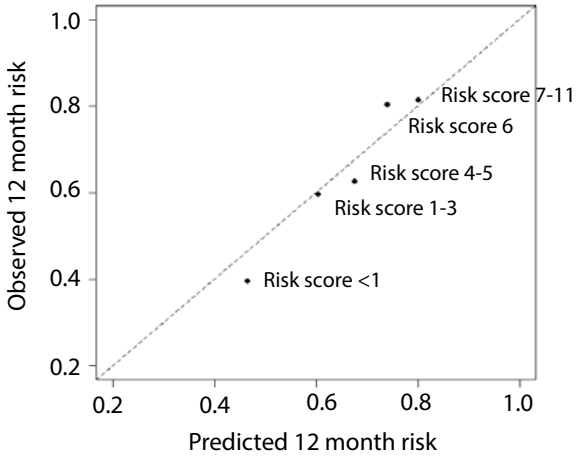

SUPPLEMENTARY FIGURE 1 | Calibration plot of the Cox proportional hazards model for the observed versus predicted risk of death at 12-months follow-up.

The dotted line represents the line of identity that presents 'the perfect model'. Each data point corresponds with a risk score interval.

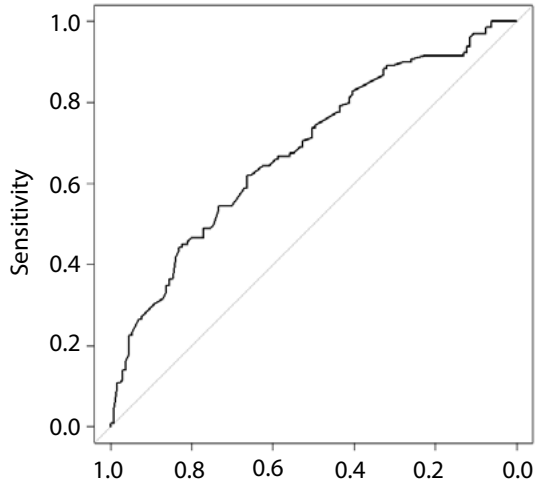

SUPPLEMENTARY FIGURE 2 | The receiver operating characteristic curve (ROC) of the multivariate Cox proportional-hazards analysis for the prediction of 12-months risk of death in DIPG is presented after applying the shrinkage factor resulting from bootstrapping.

The area under the ROC is 0.68 (95% CI 0.62-0.75).

SUPPLEMENTARY TABLE 1 | Results from multivariate Cox proportional hazards analysis in the subgroup of patients aged 3-18 years receiving radiotherapy.

Predictor	Hazard ratio (95% CI)	*P*	Coefficient
Symptom duration, mo		.018	-0.076
Ring enhancement		.037	0.302
Extension into the medulla		.005	0,415
Chemotherapy:		.009	
- Oral chemotherapy		.003	-0.489
- Intensive chemotherapy		.006	-0.456

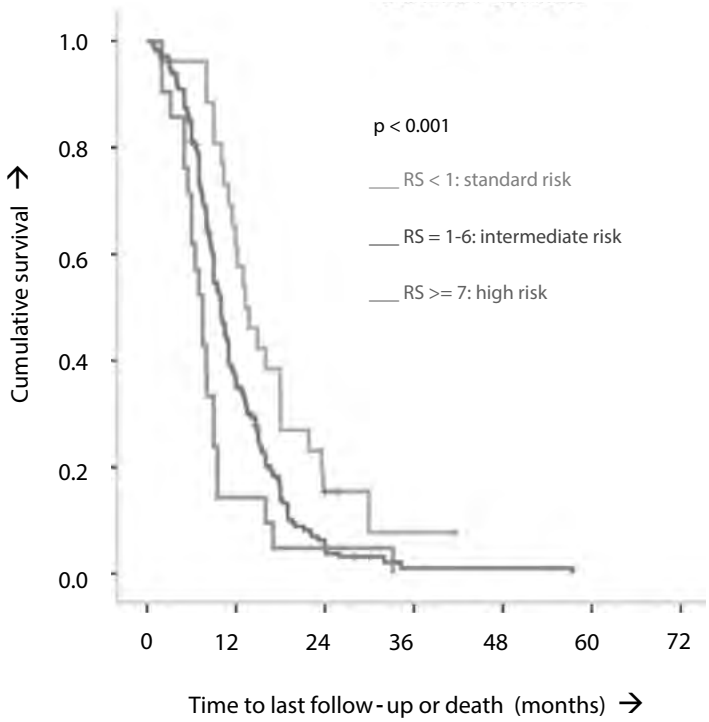

SUPPLEMENTARY FIGURE 3 | Kaplan-Meier estimates of the DIPG risk score in the DIPG subgroup of patients aged ≥3 and treated with radiotherapy.

The increasing risk score categories within this subgroup correlate with decreasing overall survival time (log rank $P < 0.001$ and generalized Wilcoxon $P < 0.0001$).

REFERENCES

[1] Grill J, Bhangoo R. Recent development in chemotherapy of paediatric brain tumours. Curr Opin Oncol. 2007;19:612–15.

[2] Hargrave D, Bartels U, Bouffet E. Diffuse brainstem glioma in children: critical review of clinical trials. Lancet Oncol. 2006;7:241–48.

[3] Jansen MH, van Vuurden DG, Vandertop WP, et al. Diffuse intrinsic pontine gliomas: a systematic update on clinical trials and biology. Cancer Treat Rev. 2012;38:27–35.

[4] Barkovich AJ, Krischer J, Kun LE, et al. Brain stem gliomas: a classifi tion system based on magnetic resonance imaging. Pediatr Neurosurg. 1990;16:73–83.

[5] Jansen MH, Kaspers GJ. A new era for children with diffuse intrinsic pontine glioma: hope for cure? Expert Rev Anticancer Ther. 2012;12:1109–12.

[6] Hargrave D, Chuang N, Bouffet E. Conventional MRI cannot predict survival in childhood diffuse intrinsic pontine glioma. J Neurooncol. 2008;86:313–19.

[7] Hipp SJ, Steffen-Smith E, Hammoud D, et al. Predicting outcome of children with diffuse intrinsic pontine gliomas using multiparametric imaging. Neuro Oncol. 2011;13:904–9.

[8] Liu AK, Brandon J, Foreman NK, et al. Conventional MRI at presentation does not predict clinical response to radiation therapy in children with diffuse pontine glioma. Pediatr Radiol. 2009;39:1317–20.

[9] Poussaint TY, Kocak M, Vajapeyam S, et al. MRI as a central component of clinical trials analysis in brainstem glioma: a report from the Pediatric Brain Tumor Consortium (PBTC). Neuro Oncol. 2011;13:417–27.

[10] Broniscer A, Laningham FH, Sanders RP, et al. Young age may predict a better outcome for children with diffuse pontine glioma. Cancer. 2008;113:566–72.

[11] Ueoka DI, Nogueira J, Campos JC, et al. Brainstem gliomas - retrospective analysis of 86 patients. J Neurol Sci. 2009;281:20–23.

[12] Harrell FE Jr., Lee KL, Mark DB. Multivariable prognostic models: issues in developing models, evaluating assumptions and adequacy, and measuring and reducing errors. Stat Med. 1996;15:361–87.

[13] Heymans MW, Anema JR, Van Buuren S, et al. Return to work in a cohort of low back pain patients: development and validation of a clinical prediction rule. J Occup Rehabil. 2009;19:155–65.

[14] Spijker J, De Graaf R, Ormel J, et al. The persistence of depression score. Acta Psychiatr Scand. 2006;114:411–16.

[15] Efron B. Bootstrap methods: another look at the jackknife. Ann Statist. 1979;7:1–26.

[16] Butler AR, Horii SC, Kricheff II, Shannon MB, Budzilovich GN. Computed tomography in astrocytomas. A statistical analysis of the parameters of malignancy and the positive contrast-enhanced CT scan. Radiology. 1978;129:433–39.

[17] Jackson S, Patay Z, Howarth R, et al. Clinico-radiologic characteristics of long-term survivors of diffuse intrinsic pontine glioma. J Neurooncol. 2013;114:339–44.

[18] Wagner S, Warmuth-Metz M, Emser A, et al. Treatment options in childhood pontine gliomas. J Neurooncol. 2006;79:281–87.

[19] Chitnavis B, Phipps K, Harkness W, Hayward R. Intrinsic brainstem tumours in childhood: a report of 35 children followed for a minimum of 5 years. Br J Neurosurg. 1997;11:206–9.

[20] Farmer JP, Montes JL, Freeman CR, et al. Brainstem Gliomas. A 10-year institutional review. Pediatr Neurosurg. 2001;34:206–14.

[21] Fisher PG, Breiter SN, Carson BS, et al. A clinicopathologic reappraisal of brain stem tumor classification. Identification of pilocystic astrocytoma and fibrillary astrocytoma as distinct entities. Cancer. 2000;89:1569–76.

[22] Kansal S, Jindal A, Mahapatra AK. Brain stem glioma - a study of 111 patients. Indian J Cancer. 1999;36:99–108.

[23] Rosenthal MA, Ashley DM, Drummond KJ, et al. Brain stem gliomas: patterns of care in Victoria from 1998–2000. J Clin Neurosci. 2008;15:237–40.

[24] Selvapandian S, Rajshekhar V, Chandy MJ. Brainstem glioma: comparative study of clinico-radiological presentation, pathology and outcome in children and adults. Acta Neurochir. 1999;141:721–26.

[25] Villani R, Gaini SM, Tomei G. Follow-up study of brain stem tumors in children. Childs Brain. 1975;1:126–35.

[26] Dellaretti M, Reyns N, Touzet G, et al. Diffuse brainstem glioma: prognostic factors. J Neurosurg. 2012;117:810–14.

[27] Wolff JE, Driever PH, Erdlenbruch B, et al. Intensive chemotherapy improves survival in pediatric high-grade glioma after gross total resection: results of the HIT-GBM-C protocol. Cancer. 2010;116:705–12.

[28] Cohen KJ, Heideman RL, Zhou T, et al. Temozolomide in the treatment of children with newly diagnosed diffuse intrinsic pontine gliomas: a report from the Children's Oncology Group. Neuro Oncol. 2011;13:410–16

[29] Yamasaki F, Kurisu K, Kajiwara Y, et al. Magnetic resonance spectroscopic detection of lactate is predictive of a poor prognosis in patients with diffuse intrinsic pontine glioma. Neuro Oncol. 2011;13:791–801.

[30] Zukotynski KA, Fahey FH, Kocak M, et al. Evaluation of 18F-FDG PET and MRI associations in pediatric diffuse intrinsic brain stem glioma: a report from the Pediatric Brain Tumor Consortium. J Nucl Med. 2011;52:188–95.

[31] Paugh BS, Broniscer A, Qu C, et al. Genome-Wide Analyses Identify Recurrent Amplifications of Receptor Tyrosine Kinases and Cell-Cycle Regulatory Genes in Diffuse Intrinsic Pontine Glioma. J Clin Oncol. 2011;29:3999–4006 .

[32] Wu G, Broniscer A, McEachron TA, et al. Somatic histone H3 alterations in pediatric diffuse intrinsic pontine gliomas and non-brainstem glioblastomas. Nat Genet. 2012;44:251–253.

[33] Khuong-Quang DA, Buczkowicz P, Rakopoulos P, et al. K27M mutation in histone H3.3 defines clinically and biologically distinct subgroups of pediatric diffuse intrinsic pontine gliomas. Acta Neuropathol. 2012;124:439–447.